Ocean Sci. Discuss., https://doi.org/10.5194/os-2017-57
Manuscript under review for journal Ocean Sci.
Discussion started: 20 July 2017

Using kinetic energy measurements from altimetry to detect shifts in the positions of fronts in the Southern Ocean

Don P. Chambers[1]

[1] College of Marine Science, University of South Florida, St. Petersburg, FL

Correspondence to: D. Chambers (donc@usf.edu)

Abstract. A novel analysis is performed utilizing cross-track kinetic energy (CKE) computed from sea surface height anomalies derived from along-track satellite altimetry. The mid-point of enhanced kinetic energy averaged over three-year periods from 1993 to 2015 is determined across the Southern Ocean and examined to detect shifts in frontal positions, based on previous observations that kinetic energy is largest along fronts and jets in the Antarctic Circumpolar Current system. It is demonstrated that although the CKE does not represent the full eddy kinetic energy (computed from crossovers), the shape of the enhanced regions along groundtracks is the same, and CKE has a much finer spatial sampling of 6.9 km. Results indicate no significant shift in the front positions across the Southern Ocean, on average, although there are some localized, large movements. This is consistent with other studies utilizing sea surface temperature gradients and the latitude of mean transport, but inconsistent with studies utilizing the movement of contours of dynamic topography.

Ocean Sci. Discuss., https://doi.org/10.5194/os-2017-57
Manuscript under review for journal Ocean Sci.
Discussion started: 20 July 2017

1. INTRODUCTION

There is as much we don't know about the circulation of the Southern Ocean as we do. Although the current system is routinely called the Antarctic Circumpolar Current (ACC), it consists of several fronts with distinct water properties to the north and south of the fronts (Nowlin and Clifford, 1982; Orsi et al., 1995; Belkin and Gordon, 1996). The most significant of these, responsible for the majority of the ACC volume transport (e.g., Cunningham et al., 2003), are the Subantarctic Front (SAF) and the Polar Front (PF). However, we now know the circulation along these fronts is not a well-defined single current, but instead consists of anywhere from three to four narrow jets per front that are highly variable in strength and location (Sokolov and Rintoul, 2007, 2009a, 2009b; Sallee et al., 2008; Thompson et al., 2010; Thompson and Richards, 2011; Langlais et al., 2011; Graham et al., 2012; Gille, 2014; Kim and Orsi, 2014).

An open question is how the fronts/jets that comprise the ACC will respond in a warming climate. Analysis of climate models suggests that as the atmosphere warms, the winds that drive the fronts/jets of the ACC will migrate south (e.g., Fyfe and Saenko, 2006; Swart and Fyfe, 2012). It should be noted, however, that the mean position of the southern hemisphere westerlies in the models lies significantly equatorward of the true position. Thus, it is not entirely clear whether the model is predicting a true shift in the wind position, or whether the model has not yet reached equilibrium with winds in the proper location.

Still, based on these model results, researchers have been testing a hypothesis that as winds in the Southern Ocean shift south, the frontal positions and jets will also migrate south. So far, the results are mixed. Sokolov and Rintoul (2009a, 2009b) proposed a method based on finding the contour of a mean dynamic topography associated with the steepest meridional gradient of

Ocean Sci. Discuss., https://doi.org/10.5194/os-2017-57
Manuscript under review for journal Ocean Sci.
Discussion started: 20 July 2017

dynamic topography (i.e., zonal geostrophic current) and associate this with a front or jet. They could then track the latitude of that contour over time to deduce if the front had moved. When averaged over all longitudes, their analysis indicated that the SAF and PF had both moved south by approximately 60 km over 15 years (Sokolov and Rintoul, 2009b).

While this method is nice because it allows one to determine a front position even when gradients are small due to continuity of the contour line and is less contaminated with errors such as those based on methods that examine gradients alone (e.g., Chapman, 2014), it has several issues because of several assumptions made. First, it assumes that the average of the position shift of the contours across all longitudes represents the shift at all longitudes. Kim and Orsi (2014) recently considered this assumption and found that while the average frontal position indicates a strong southward shift, this is due to substantial shifts only in the Indian Ocean sector. There are no significant shifts throughout the Pacific or Atlantic Ocean sectors.

The second assumption assumes that a contour of dynamic topography shifting south is unique to a front/jet axis moving south. This is not true. Gille (2014) demonstrated that all contours in the Southern Ocean have shifted south on average, and that this follows from the observed rise in sea level – as the sea surface height rises, the contours will appear to shift south. Gille (2014) used a different measure to determine the position of the ACC fronts, based on the latitude of the mean surface transport of the ACC measured by altimetry, and found no significant shift but considerable interannual variability.

The third assumption is that the front/jet position has shifted south but that the magnitude and width of the jet has not changed. The problem with this assumption is demonstrated in **Figure 1**, where we show the mean dynamic topography (MDT) from two jet scenarios: 1) where the peak of two Gaussian shaped jets have shifted south, and 2) where the peak has not shifted, but the

Ocean Sci. Discuss., https://doi.org/10.5194/os-2017-57
Manuscript under review for journal Ocean Sci.
Discussion started: 20 July 2017

magnitude has decreased, the width has broadened, and the shape has become slightly skewed. Although the resulting MDT profiles are not identical, they are similar, and both suggest a southward movement of MDT contours.

Researchers using other methods also find little or no southern migration of the fronts or jets in the Southern Ocean as a whole. Graham et al. (2012) used a high-resolution model to show that the Polar Front and Subantarctic Front are constrained by bathymetry, even in increasing and shifting winds. Freeman et al. (2016) used weekly estimates of the Polar Front position determined from satellite sea surface temperature (SST) measurements to show no significant southward shift, except in the Indian Ocean (similar to Kim and Orsi, 2014) and a northward shift in part of the south Pacific.

Here, we will utilize a new method to study the position of the fronts in the Southern Ocean, based on tracking the location of eddy kinetic energy (EKE) measured by altimetry. It is known from modeling studies that the front positions are associated with increased EKE, due to instabilities in the jets and interactions with bathymetry (Thompson et al., 2010; Thompson and Richards, 2011). Thus, it is reasonable to assume that if the front position has shifted that the region of high EKE should also shift by a comparable amount.

2. DATA AND METHODS

We will utilize geostrophic surface current anomalies computed from the 23-year record from the TOPEX/Poseidon, Jason-1, and Jason-2 1-Hz sea surface height (SSH) data along each groundtrack in the Southern Ocean (**Figure 2**). We utilize this record rather than the gridded products based on mapping SSH from multiple altimeters (e.g., Ducet et al., 2000), because the along-track data high have a finer resolution in space (6.9 km along the groundtrack) and Hogg et al. (2015) demonstrated that the mapped altimetry data underestimated EKE due to attenuation from the large-scale correlation functions used in the mapping procedure.

The altimetry data used are from three separate altimeter missions: TOPEX/Poseidon (January 1993 – January 2002), Jason-1 (February 2002 – July 2008), and Jason-2 (August 2008 – December 2015). Because the official TOPEX/Poseidon (T/P) geophysical data records (GDRs) have not been updated since the late 1990s, we utilize the corrected data products from the Integrated Multi-Mission Ocean Altimeter Data for Climate Research provided by Beckley et al. (2010) at the NASA PO.DAAC site (https://podaac.jpl.nasa.gov/Integrated_Multi-Mission_Ocean_AltimeterData). Jason-1 data are from the GDR-C version and were downloaded from the NASA PO.DAAC site in June 2010. Jason-2 are from the GDR-D version and were downloaded from NOAA NODC (ftp://ftp.nodc.noaa.gov/pub/data.nodc/jason2) between August 2012 and June 2016. We utilize the 1-Hz along-track data from the three altimeters and interpolate to the same fixed ground track utilizing the DTU10 mean sea surface model (Andersen and Knudsen, 2009; http://www.space.dtu.dk/english/Research/Scientific_data_and_models/downloaddata). All recommended geophysical and surface corrections (e.g., water vapor, ionosphere, sea state bias, ocean tides, inverted barometer, etc) have been applied. SSH anomalies are computed by subtracting the DTU10 mean sea surface model from the interpolated SSH data.

The time-varying, anomalous geostrophic current normal to the groundtrack (u_T) can be computed directly from the derivative of the SSH anomaly (η) along the ground-track distance (dr) from

$$u_T = \frac{g}{f}\frac{d\eta}{dr}, \tag{1}$$

where g is the acceleration due to gravity, and f is the Coriolis parameter. This cross-track current is a projection of both the zonal (u) and meridional (v) components of the full velocity field. However, neither u nor v can be determined unambiguously from u_T without significant simplifying assumptions. Here, we merely examine the variability of u_T without making any assumptions concerning how it may be related to the full velocity, or u and v.

Because derivatives have to be computed numerically (here, center-differences are used) and η contains significant noise at the 1 Hz sampling-rate of the altimeters, we chose to optimally interpolate η along-track using a model of the covariance of the signal and error. We used the method of Wunsch (2006, Chapter 3) and a covariance function modeled as a Gaussian with a roll-off of 98 km and random noise of 2 cm, which was determined from the autocovariance of all TOPEX/Poseidon, Jason-1, and Jason-2 SSHA data from 1993-2015 between 40°S and 65°S.

Once $u_T(t)$ was computed at each 1-sec bin along the groundtracks in Figure 2 for each 10-day repeat cycle, the cross-track kinetic energy (CKE) was computed as CKE(x,t) = 0.5 $u_T(x,t)^2$, where x here is used to denote a generic 1-sec bin along the ground track. These CKE values were averaged over the entire 23-year record and examined for each groundtrack segment (both ascending and descending) to judge where CKE was exceptionally high (Figure 3). We also computed CKE using the raw values of η with no optimal interpolation and compared to that computed with optimal interpolation. The locations of high CKE were the same, although values were slightly higher with the unsmoothed data. The quiescent regions of the ocean also showed considerably more noise, making it more difficult to determine boundaries of elevated CKE. For this reason, the values determined from the optimally interpolated data were used.

Several criteria were utilized to quantify where the high CKE values were considered to be associated with fronts or jets. First, we constrained the southern boundary to be 5° south of the

Ocean Sci. Discuss., https://doi.org/10.5194/os-2017-57
Manuscript under review for journal Ocean Sci.
Discussion started: 20 July 2017

Orsi et al. (1995) values of the PF and the northern boundary to be 5° north of the SAF. Secondly, we used a lower-limit for CKE of 200 cm^2 s^{-2} for detection; only values higher than this were considered high and likely associated with a front. For the example shown in Figure 3 (from a track in the south Indian Ocean), there is a region of CKE greater than 200 cm^2 s^{-2} between 55°S and 47°S. The value of 200 cm^2 s^{-2} was chosen over a lower value because it was found that the regions selected with the 200 cm^2 s^{-2} were consistent from one 10-day period to another. Using lower minimum values resulted in areas of high CKE activity being detected in some cycles, but not others. An example is the small rise in mean CKE at 41°S in Figure 3. Although the mean CKE is about 150 cm^2 s^{-2}, suggestive of a jet, this all but disappears for some periods of time. This behavior of jets has been observed in models (e.g., Thompson and Richards, 2011). Thus, the minimum CKE was selected to be as conservative as possible.

The mean CKE profile pictured in Figure 3 has multiple local maxima, most likely associated with the narrow jets that surround the front. Most of the other profiles examined had similar features. We initially tried tracking each of the maxima, but that quickly became complicated because sometimes the four or local maxima would become five, or even just one. This is likely due to the instability of the jets around the front. In order to ensure consistency and assuming the mean of the region of high CKE followed the front position, the half-power point, or centroid, of the CKE bump was computed. This is similar in principle to the computation made by Gille (2014) of the latitude of the mean ACC transport, except here we are focused on mean of the CKE around a particular front, not over all the fronts of the ACC.

To compute the half-power point, a southern and northern boundary of the CKE bump had to be determined. These were computed by first finding the maximum of CKE in the bump, then finding the first value to the north just below 25% of that peak along with the similar value to the

Ocean Sci. Discuss., https://doi.org/10.5194/os-2017-57
Manuscript under review for journal Ocean Sci.
Discussion started: 20 July 2017

south (shown in Figure 3). These were selected as the north (x_{north}) and south (x_{south}) boundaries for the calculation of the half-power point (x_{mid}) so that

$$\int_{x_{south}}^{x_{mid}} CKE(x)\,dx = \frac{1}{2}\int_{x_{south}}^{x_{north}} CKE(x)\,dx\,. \tag{2}$$

Values other than 25% of the peak were tested. Using value greater than this, up to 50%, resulted in no significant difference in the half-power point. Using values smaller resulted in some boundaries not being defined. Thus, 25% of peak CKE was considered reasonable. If multiple regions of enhanced CKE were found along the same track, this process was carried out for each of them. This was done for all the mean CKE profiles to establish the mean locations of the fronts between 1993 and 2015.

A similar procedure was done for CKE averaged over discrete 3-year intervals, starting in 1993. This provided 8 distinct samples of CKE for each groundtrack from which to deduce shifts in the half-power point.

3. RESULTS AND ANALYSIS

The first thing tested was how well CKE represented the full EKE, where EKE = $0.5(u^2 + v^2)$. One can calculate both components of the velocity at crossover points, where the ascending and descending groundtracks cross, under the assumption that the velocity field has not changed significantly between the times of the groundtracks (Parke et al., 1987). At high latitudes of the Southern Ocean, the time separation between ascending and descending passes is less than 3 days for 78% of the crossovers, so this is a reasonable assumption.

Ocean Sci. Discuss., https://doi.org/10.5194/os-2017-57
Manuscript under review for journal Ocean Sci.
Discussion started: 20 July 2017

Knowing the groundtrack angle with the north meridian (θ) one can compute the zonal ($d\eta/dy$) and meridional gradients ($d\eta/dx$) of SSHA directly from the gradients of SSHA for the ascending pass ($d\eta/dr_{asc}$) and descending pass ($d\eta/dr_{des}$) using simple geometry

$$\frac{d\eta}{dy} = \frac{\left[\frac{d\eta}{dr_{asc}} - \frac{d\eta}{dr_{des}}\right]}{2\sin\theta}, \frac{d\eta}{dx} = \frac{\left[\frac{d\eta}{dr_{asc}} + \frac{d\eta}{dr_{des}}\right]}{2\cos\theta}, \tag{3}$$

noting that this formulation assumes the gradients represent the derivative of the northern SSHA relative to the southern SSHA (for both the ascending and descending passes). Once this is computed, the velocities can be computed directly from the zonal and meridional gradients:

$$u = -\frac{g}{f}\frac{d\eta}{dy}, v = \frac{g}{f}\frac{d\eta}{dx}. \tag{4}$$

Although CKE is lower than EKE along all groundtracks (see Figure 4 for examples), the pattern of KE rise then fall is virtually identical. CKE, however, has the benefit of higher and more regular sampling. Thus, we conclude CKE is a reasonable proxy for locating front positions even though it may not be useful for quantifying the full energy of the anomalous currents.

Three general types of enhanced CKE were found (Figure 4). In most regions, the “bump” in CKE is more or less symmetrical. In several, however, the bump is skewed, with a long rise then a sharp drop-off. Finally, there were also a few cases where two distinct regions of enhanced CKE were identified. In all cases, the shape of the CKE closely followed that of EKE, although the amplitude was attenuated, by anywhere from 25-50%.

Figure 2 shows the locations of the half-power points determined from the mean CKE profiles. Although a potential front position is not found along every groundtrack, they are typically found in areas where currents are strong and close to perpendicular with the ascending or descending groundtracks. It is also clear that there are more sites found along the SAF than the PF. A few are found between the two fronts, but this is likely due to either errors in the older front database of Orsi et al. (1995), changes since the hydrographic data used in that study were collected, or jets between the fronts. One location is found substantially south of the Polar Front, and is likely related to the weaker Southern ACC front.

Figure 5 shows the variability in the enhanced CKE along one groundtrack for the three-year intervals compared to the mean, and demonstrates the problem with separating the positions of the highly variable jets from the front. For example, in 1999-2001, there were 6 distinct local maxima of CKE (indicated by blue dots), suggesting jets. In 2002-2004, there were also 6 (indicated by orange dots), but in different locations. Does this indicate a movement of the jet, or a new one? That is impossible to say without making considerable assumptions, which is why we only consider the movement of the half-power point of enhanced CKE as defined in Section 2.

To quantify potential movement, a linear trend is fit to the 8 estimations of the half-power point from 1993-2015 for each location shown in Figure 2. Analysis of the residuals about the trend indicated they were random (lag-1 autocorrelation < 0.1 for all cases), so standard error was computed by scaling the formal error from ordinary least squares by the standard deviation of the residuals. This was also scaled up to account for the degrees of freedom lost by estimating the trend (making the effective degrees of freedom 6) by scaling by sqrt(8/6). Finally, the 90% confidence interval was computed by scaling by 1.94 for 6 effective degrees of freedom assuming a normal t-distribution.

The results indicate considerable regional variability in the change of the half-power point over 23 years, with large uncertainty bars (Figure 6). This is due to the substantial temporal variability in the position, which can be seen somewhat in Figure 5, where the leading edge of the CKE bump varies by over 1 degree of latitude (over 100 km) between 1993-1995 and 2011-2012. To better see significant changes outside the uncertainty (90% confidence) interval, one can compute the signal to noise ratio (SNR = trend/uncertainty). Examining this (Figure 7), one can see there are some regions where the half-power point has moved southward by a significant distance over the last 23 years (13.6% of points), but there are also points where it has moved north (9.6%). For the majority of points (76.8%), there is no significant change

4. DISCUSSION AND CONCLUSIONS

The results from the analysis of the positions of enhanced kinetic energy suggest no overall shift in the front positions across the Southern Ocean, but some large, localized movements. The region indicative of some southward shifts between 90°E and 170°E is in approximately the same area where Kim and Orsi (2014) and Freeman et al. (2016) also reported large shifts. However Freeman et al. only examined the Polar front, and Kim and Orsi (2014) only found large shifts in the PF and the southern ACC front. They found shifts of order 50-100 km in the SAF where the points in this study cluster. Our results suggest considerably larger shifts in some areas between 90°E and 170°E, although the overall average (-29 km per decade, or -66.7 km in 23 years), is consistent with what Kim and Orsi (2014) found.

Kim and Orsi (2014) and Freeman et al. (2016) also found slight northward shifts in the front positions in the southeast Pacific, between 200°E-270°E. We also find some locations in this region with a significant northward shift in the SAF. Kim and Orsi (2014) found the shift of the SAF was about 30-40 km between 1992 and 2011. Our results suggest larger shifts in some areas; averaged over the area, our results are 46 km per decade to the north, or 106 km from

Ocean Sci. Discuss., https://doi.org/10.5194/os-2017-57
Manuscript under review for journal Ocean Sci.
Discussion started: 20 July 2017

1993-2015, which is consistent with the average over the region computed by Freeman et al. (2016) from sea surface temperature data, but for the Polar Front.

Overall, this study supports the recent studies by Kim and Orsi (2014), Gille (2014), and Freeman et al. (2016) that the frontal positions of the ACC are highly variable in time and that there is no statistically significant shift in the fronts to the south on average. This study utilized a novel technique to reach this conclusion, which adds to the robustness of evidence that there has not been a shift in the frontal positions. Thus, while the fronts may eventually shift south in a warming climate, there is no strong evidence that it is happening at the moment.

The only evidence supporting this hypothesis comes from mapping the location of contours of constant dynamic topography over time (e.g., Sokolov and Rintoul, 2009b; Kim and Orsi, 2014). As Gille (2014) argued and as we have demonstrated based on a simple thought experiment (Figure 1), there are other equally plausible explanations for the apparent southern shift of the contours. Considering that three different techniques – location of mean transport (Gille, 2014), maximum SST gradients (Freeman et al., 2016), and location of enhanced kinetic energy (this study) – all agree that the fronts have not moved significantly on average, one has to conclude that the method of using dynamic topography contours to detect changes in front position is flawed. As Gille (2014) concluded, the most likely explanation for the signal is the observed rise in sea level over the region due to warming of water in the region.

Acknowledgements

This research was carried out under grant number NNX13AG98G from NASA and Grant number *** from NOAA for the NASA/NOAA Ocean Surface Topography Science Team.

REFERENCES

Andersen O B, and Knudsen P: DNSC08 mean sea surface and mean dynamic topography models, *J. Geophys. Res.*, *114*, C11001, doi:10.1029/2008JC005179, 2009.

Beckley, B.D., Zelensky, N.P., Holmes, S.A., Lemoine, F.G., Ray, R.D., Mitchum, G.T., Desai, S., and Brown, S. T.: Assessment of the Jason-2 Extension to the TOPEX/Poseidon, Jason-1 Sea-Surface Height Time Series for Global Mean Sea Level Monitoring, *Marine Geodesy, 33*(S1): 447-471, Supplemental Issue on OSTM/Jason-2 calibration/validation, Vol. 1, DOI: 10.1080/01490419.2010.491029, 2010

Belkin, I. M., and Gordon, A. L.: Southern Ocean fronts from the Greenwich meridian to Tasmania, J. Geophys. Res., 101, 3675–3696, 1996.

Chapman, C. C.: Southern Ocean jets and how to find them: Improving and comparing common jet detection methods, J. Geophys. Res. Oceans, 119, 4318–4339, doi:10.1002/2014JC009810, 2014.

Cunningham, S. A., Alderson, S. G. , King, B. A., and Brandon, M. A.: Transport and variability of the Antarctic Circumpolar Current in Drake Passage, J. Geophys. Res., 108(C5), 8084, doi:10.1029/2001JC001147, 2003

Dong, S., Sprintall, J., and Gille, S. T. : Location of the Antarctic Polar Front from AMSR-E Satellite Sea Surface Temperature measurements, J. Phys. Oceanogr., 36, 2075–2089, doi:10.1175/JPO2973.1, 2006.

Ducet, N., Le Traon, P.-Y., Reverdin, G.: Global high resolution mapping of ocean circulation from TOPEX/Poseidon and ERS-1 and -2. Journal of Geophysical Research 105 (C8), 19477–19498, 2000.

Fyfe, J. C., and Saenko, O. A.: Simulated changes in the extratropical Southern Hemisphere winds and currents, Geophys. Res. Lett., 33, L06701, doi:10.1029/2005GL025332, 2006.

Gille, S. T.: Meridional displacement of the Antarctic Circumpolar Current, Philos. Trans. R. Soc. A, 372, 20130273, doi:10.1098/rsta.2013.0273, 2014.

Graham, R. M., De Boer, A. M., Heywood, K. J., Chapman, M. R., and Stevens, D. P.: Southern Ocean fronts: Controlled by wind or topography?, J. Geophys. Res. Oceans, 117, C08018, doi:10.1029/2012JC007887, 2012.

Hogg, A. McC., Meredith, M. P., Chambers, D. P., Abrahamsen, E. P., Hughes, C. W., and Morrison, A. K.: Recent trends in the Southern Ocean eddy field, J. Geophys. Res. Oceans, 120, 257–267, doi:10.1002/2014JC010470, 2015.

Kim, Y. S., and Orsi, A. H.: On the variability of Antarctic Circumpolar Current fronts inferred from 1992-2011 altimetry, J. Phys. Oceanogr., 44, 3054–3071, doi:10.1175/JPO-D-13-0217.1, 2014.

Ocean Sci. Discuss., https://doi.org/10.5194/os-2017-57
Manuscript under review for journal Ocean Sci.
Discussion started: 20 July 2017

Ocean Science Discussions

Langlais, C., Rintoul, S. R., and Schiller, A.: Variability and mesoscale activity of the Southern Ocean fronts: Identification of a circumpolar coordinate system, Ocean Modell., 39, 79–96, doi:10.1016/j.ocemod.2011.04.010, 2011.

Moore, J. K., Abbott, M. R., and Richman, J. G.: Location and dynamics of the Antarctic Polar Front from satellite sea surface temperature data, J. Geophys. Res., 104, 3059–3073, doi:10.1029/1998JC900032, 1999.

Nowlin, W. D., and Clifford, M.: The kinematic and thermohaline zonation of the Antarctic Circumpolar current at Drake Passage, J. Mar. res., 40, 481-507, 1995.

Orsi, A. H., Whitworth III, T., and Nowlin Jr., W. D.: On the meridional extent and fronts of the Antarctic Circumpolar Current, Deep Sea Res., Part I, 42(5), 641–673, doi:10.1016/0967-0637(95)00021-W, 1995.

Parke, M. E., Stewart, R. H. , Farless, D. L., and Cartwright, D. E.: On the choice of orbits for an altimetric satellite to study ocean circulation and tides, J. Geophys. Res., 92, 11693–11707, 1987.

Sallee, J. B., Speer, K., and Morrow, R.: Response of the Antarctic Circumpolar Current to atmospheric variability, J. Clim., 21(12), 3020–3039, doi:10.1175/2007JCLI1702.1, 2008.

Sokolov, S., and Rintoul, S. R.: Multiple jets of the Antarctic Circumpolar Current south of Australia, J. Phys. Oceanogr., 37, 1394–1412,doi:10.1175/JPO3111.1, 2007.

Sokolov, S., and Rintoul, S. R.: Circumpolar structure and distribution of the Antarctic Circumpolar Current fronts: 1. Mean circumpolar paths, J. Geophys. Res., 114, C11018, doi:10.1029/2008JC005108, 2009a.

Sokolov, S., and Rintoul, S. R.: Circumpolar structure and distribution of the Antarctic Circumpolar Current fronts: 2. Variability and relationship to sea surface height, J. Geophys. Res., 14, C11019, doi:10.1029/2008JC005248, 2009b.

Swart, N., and Fyfe, J. C.: Observed and simulated changes in the Southern Hemisphere surface westerly wind-stress. Geophys. Res. Lett., 39, L16711, doi:10.1029/2012GL052810, 2012.

Thompson, A. F., Haynes, P. H., Wilson, C., and Richards, K. J.: Rapid Southern Ocean front transitions in an eddy-resolving ocean GCM, Geophys. Res. Lett., 37, L23602, doi:10.1029/2010GL045386, 2010.

Thompson, A. F., and Richards, K. J.: Low frequency variability of Southern Ocean jets, J. Geophys. Res., 116, C09022, doi:10.1029/2010JC006749, 2011.

Wunsch, C.: *The Ocean Circulation Inverse Problem*, 458 pp., Cambridge Univ. Press, Cambridge, Mass.

Ocean Sci. Discuss., https://doi.org/10.5194/os-2017-57
Manuscript under review for journal Ocean Sci.
Discussion started: 20 July 2017

Figure Captions

Figure 1. a) Mean dynamic topography in the Southern Ocean along a north-south meridian for three scenarios, and b) the corresponding geostrophic velocity, with positive values indicating eastward flow. The scenarios are: an initial state (dashed black line), a shift of the two fronts south by 60 km with no change in magnitude or shape of the currents (red line), and no shift of the mean of the current, but a change in the magnitude and shape (blue line).

Figure 2. Positions of the T/P, Jason-1, and Jason-2 groundtracks used for this study (black lines), the approximate locations of the Subantarctic Front (red line) and the Polar Front (blue line), as well as locations where enhanced cross-track kinetic energy was found (orange dots). The front positions are from Orsi et al. (1995).

Figure 3. An example profile of mean CKE along a ground track in the southern Indian Ocean, demonstrating the location of the half-power point and the locations of the southern and northern boundaries of the CKE bump. See text for details of the computations.

Figure 4. Examples of the three types of CKE profiles found (black lines), along with the value of the full EKE computed at crossover points.

Figure 5. Examples of the time-variable CKE profiles found, averaged over 3-year periods. The ground track is the same shown Figure 3 for the southern Indian Ocean. Colored dots indicate the location of probable jets in 2002-2004 (orange) and in 1999-2001 (blue).

Figure 6. Estimated trend in the half-power point of CKE for each location shown in Figure 2, as a function of latitude. Error bars represent the 90% confidence interval.

Figure 7. SNR (trend/error in Figure 6). Values larger than 1 indicate a statistically significant northern shift. Values smaller than -1 indicate a statistically significant southern shift. Values between ± 1 indicate no statistically significant shift.

Ocean Sci. Discuss., https://doi.org/10.5194/os-2017-57
Manuscript under review for journal Ocean Sci.
Discussion started: 20 July 2017

Ocean Science
Discussions

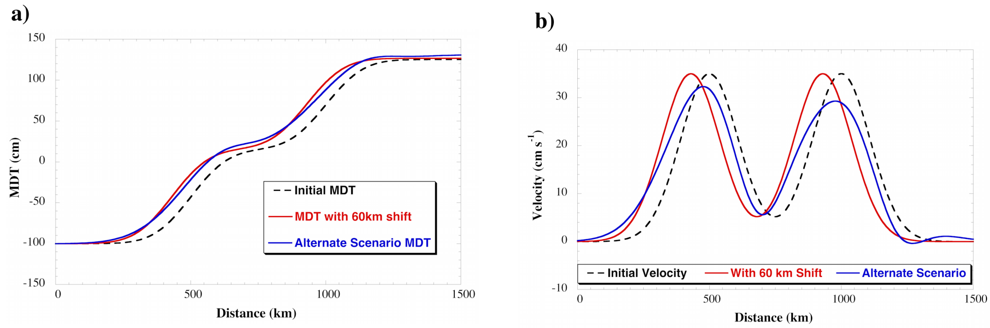

Figure 1. a) Mean dynamic topography in the Southern Ocean along a north-south meridian for three scenarios, and b) the corresponding geostrophic velocity, with positive values indicating eastward flow. The scenarios are: an initial state (dashed black line), a shift of the two fronts south by 60 km with no change in magnitude or shape of the currents (red line), and no shift of the mean of the current, but a change in the magnitude and shape (blue line).

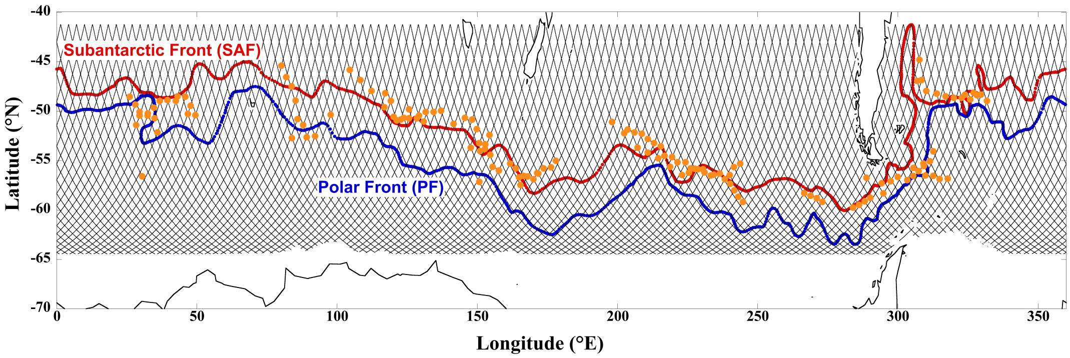

Figure 2. Positions of the T/P, Jason-1, and Jason-2 groundtracks used for this study (black lines), the approximate locations of the Subantarctic Front (red line) and the Polar Front (blue line), as well as locations where enhanced cross-track kinetic energy was found (orange dots). The front positions are from Orsi et al. (1995).

Ocean Sci. Discuss., https://doi.org/10.5194/os-2017-57
Manuscript under review for journal Ocean Sci.
Discussion started: 20 July 2017

Ocean Science
Discussions

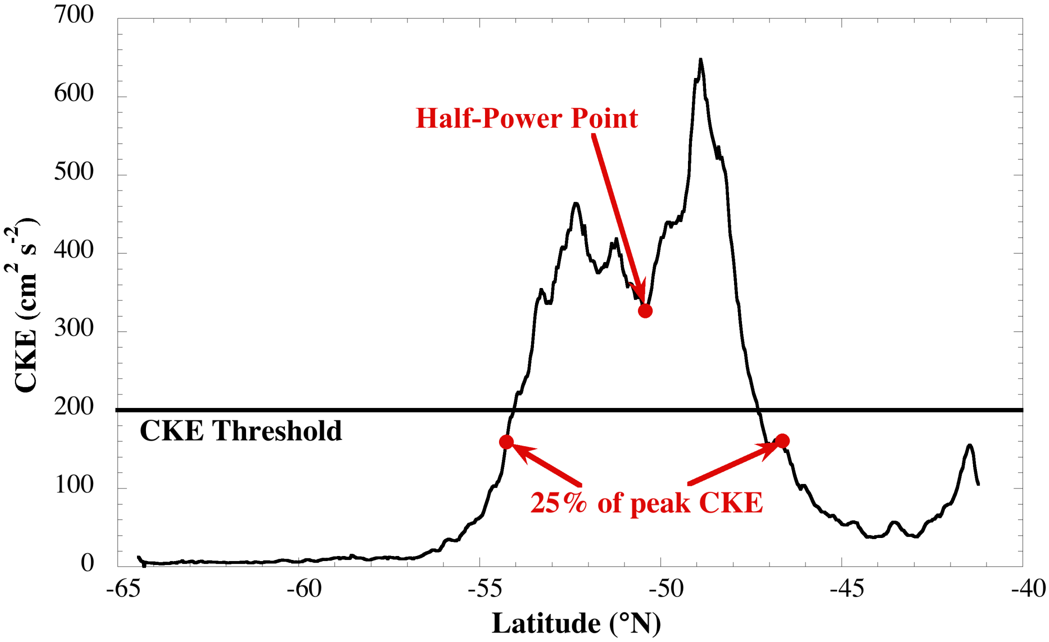

Figure 3. An example profile of mean CKE along a ground track in the southern Indian Ocean, demonstrating the location of the half-power point and the locations of the southern and northern boundaries of the CKE bump. See text for details of the computations.

Ocean Sci. Discuss., https://doi.org/10.5194/os-2017-57
Manuscript under review for journal Ocean Sci.
Discussion started: 20 July 2017

Ocean Science
Discussions
Open Access

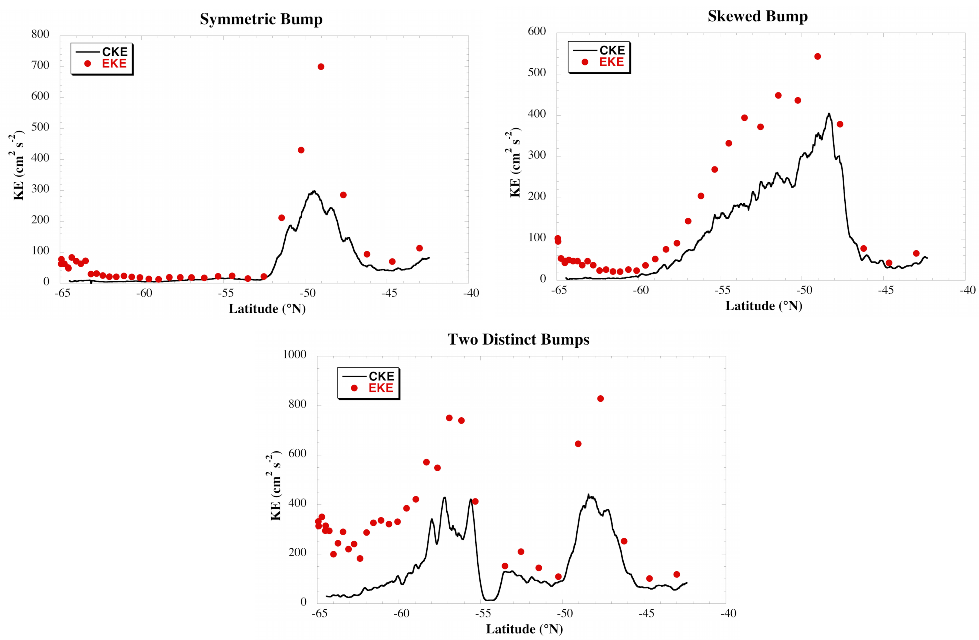

Figure 4. Examples of the three types of CKE profiles found (black lines), along with the value of the full EKE computed at crossover points.

Ocean Sci. Discuss., https://doi.org/10.5194/os-2017-57
Manuscript under review for journal Ocean Sci.
Discussion started: 20 July 2017

Ocean Science
Discussions
Open Access

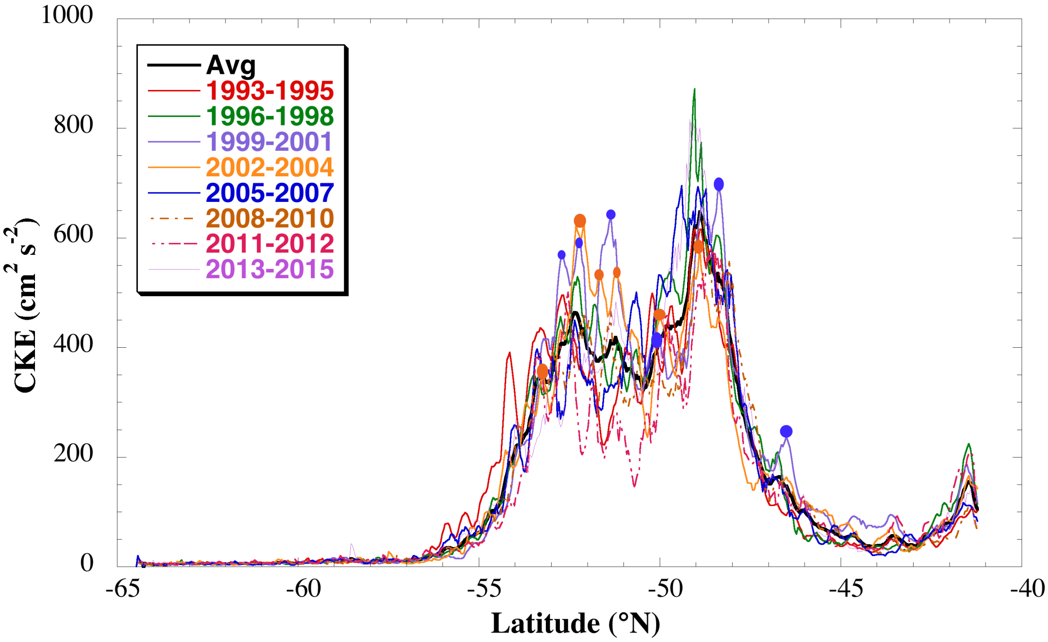

Figure 5. Examples of the time-variable CKE profiles found, averaged over 3-year periods. The ground track is the same shown Figure 3 for the southern Indian Ocean. Colored dots indicate the location of probable jets in 2002-2004 (orange) and in 1999-2001 (blue).

Ocean Sci. Discuss., https://doi.org/10.5194/os-2017-57
Manuscript under review for journal Ocean Sci.
Discussion started: 20 July 2017

Ocean Science
Discussions

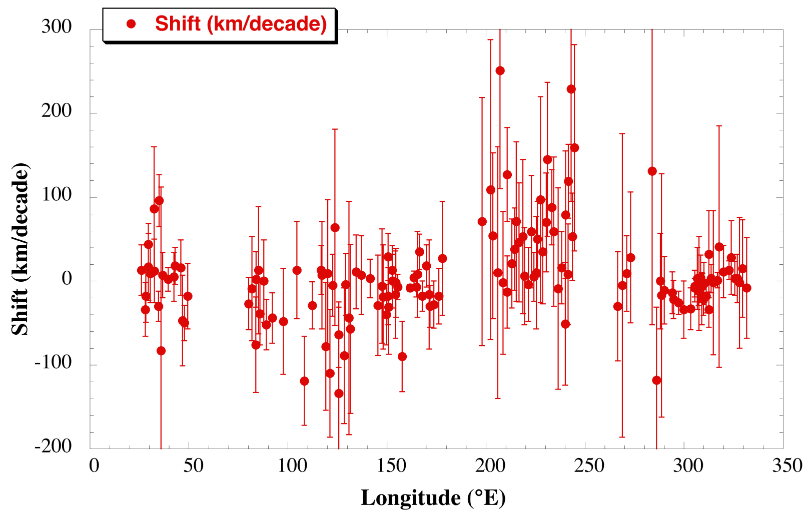

Figure 6. Estimated trend in the half-power point of CKE for each location shown in Figure 2, as a function of latitude. Error bars represent the 90% confidence interval.

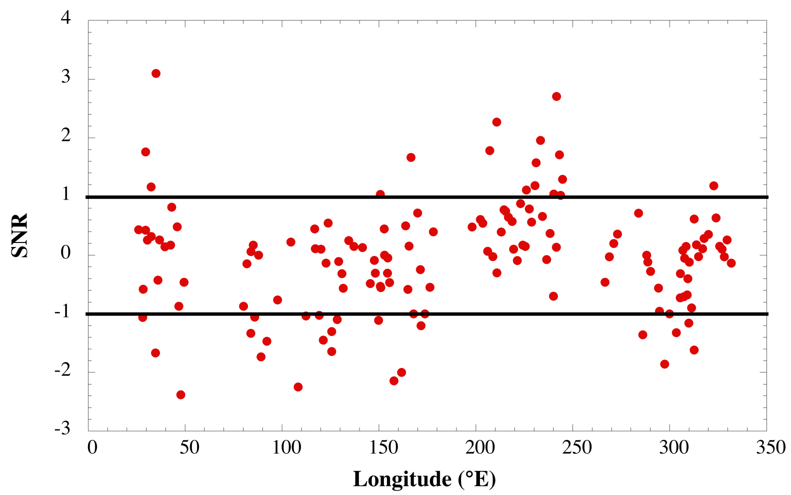

Figure 7. SNR (trend/error in Figure 6). Values larger than 1 indicate a statistically significant northern shift. Values smaller than -1 indicate a statistically significant southern shift. Values between ± 1 indicate no statistically significant shift.